Steam-Exploded Residual Softwood-Filled Polypropylene Composites

M. NEUS ANGLÈS,[1] JOAN SALVADÓ,[1] ALAIN DUFRESNE[2]

[1] Departament d'Enginyeria Química, Escola Tècnica Superior d'Enginyeria Química, Universitat Rovira i Virgili, Plaça Imperial Tarraco, 1, 43005 Tarragona, Catalonia, Spain

[2] Centre de Recherches sur les Macromolécules Végétales (CERMAV–CNRS), Université Joseph Fourier, BP 53, 38041 Grenoble cedex 9, France

Received 25 January 1999; accepted 10 May 1999

ABSTRACT: Residual softwood sawdust was pretreated by a steam-explosion technique. It was used as a natural filler in polypropylene (PP)-based composites. Dynamic mechanical analysis and tensile properties of these materials were studied. The influence of filler loading, steam-explosion severity, and coating the fiber with a functionalized compatibilizer, such as maleic anhydryde polypropylene (MAPP), on the mechanical behavior of the composite was evaluated. The results were analyzed in relation with scanning electron microscopy observations, and surface energy (dispersive and polar components) and apparent specific area measurements. Experimental data indicate a better compatibility between MAPP-coated fiber and PP with respect to the untreated one. The coating treatment of the softwood fiber was found to promote interfacial adhesion between both components, and to enhance the tensile properties of the resulting composite. This reinforcing effect was well predicted from theoretical calculations based on a mean field approach (Halpin-Kardos model). The steam-explosion pretreatment severity increased the surface energy and apparent specific surface, and resulted in a loss of the fiber entirety. The sorption behavior of these composite materials was also performed. It was found that the composites absorb more water, as the filler content is higher. MAPP coating provided protection from water uptake in the interphase region. © 1999 John Wiley & Sons, Inc. J Appl Polym Sci 74: 1962–1977, 1999

Key words: steam explosion; lignocellulosic; polypropylene composite; mechanical properties; water absorption

INTRODUCTION

Polyolefin polymers, such as polypropylene (PP), are widely used in automotive industry or for domestic applications when ductility and low cost have to be combined. In addition, mineral fillers and fibers are now extensively used in the plastics industry to achieve desired properties or to reduce the price of the finished article.

There is an increasing interest in environmental concerns. It is potenciated to maximize the use of renewable resources and also to minimize the wastes. So the valorization of a lignocellulosic residual material and its use as a lightweight and economical source of reinforcement in thermoplastic composites has received substantial attention.[1–11] Compared to inorganic fillers, the main advantages of lignocellulosics are their renewable

Correspondence to: A. Dufresne.

Contract grant sponsor: Spanish Government and Generalitat de Catalunya; contract grant numbers: GSR96 and QFN95-4720.

Contract grant sponsor: Grant of the Universitat Rovira i Virgili.

Journal of Applied Polymer Science, Vol. 74, 1962–1977 (1999)
 CCC 0021-8995/99/081962-16

nature, wide variety of fillers available throughout the world, nonfood agricultural-based economy, low energy consumption, cost and density, high specific strength and modulus, high sound attenuation of lignocellulosic-based composites, comparatively easy processability due to their nonabrasive nature, which allows high filling levels, resulting in significant cost savings, and relatively reactive surface, which can be used for grafting specific groups. Moreover, the recycling by combustion of lignocellulosic-filled composites is easier compared to inorganic fillers systems. Therefore, the possibility of using lignocellulosic fillers in the plastic industry has received considerable interest. Nevertheless, it must be taken into account that the performance of the lignocellulosics as a reinforcing filler depends on its origin and on the quality of the fiber.[4] High-performance polysaccharide-based composite materials can also be obtained using prehydrolyzed cellulose microfibrils,[12,13] cellulose whiskers,[14–16] or starch microcrystals.[17,18]

Despite these attractive properties, lignocellulosic fillers are used only to a limited extent in industrial practice due to difficulties associated with surface interactions. The inherent polar and hydrophilic nature of lignocellulosics and the nonpolar characteristics of most of thermoplastics result in difficulties in compounding the filler and the matrix, and therefore, in achieving acceptable dispersion levels, which results in inefficient composites. This hydrogen bonding is best exemplified in paper, where these secondary interactions provide the basis of its mechanical strength.

Another drawback of lignocellulosic fillers is their high moisture absorption, and the resulting swelling and decrease in mechanical properties. Moisture absorbance and corresponding dimensional changes can be largely prevented if the hydrophilic filler is thoroughly encapsulated in an hydrophobic polymer matrix and there is good adhesion between both components. However, if the adhesion level between the filler and the matrix is not good enough, diffusion pathway can preexist or can be created under mechanical solicitation. The existence of such pathway is also related to the filler connection and, therefore, to its percolation threshold.

It is well known that raw lignocellulosic materials are mainly made of a complex network of three polymers, namely cellulose, hemicelluloses, and lignin. Different pretreatments, either mechanical, thermal, or chemical, lead to a more or less successful separation with partial degradation. The steam explosion process combine these three effects and allows a rather selective separation of lignocellulosics into their individual components.[19–25] The purpose of this treatment is to remove most of the lignin and hemicelluloses, which are highly hygroscopic. Several types of steam treatment have been developed. All of them consist in keeping the raw material under vapor pressure in a reactor during a given time, but they differ from one another mainly in the way the pressure is released at the end of the treatment: fast or slowly. It was found that, after the process, the cellulose showed a higher reactivity towards chemical and biochemical reagents.[26] The extraction step of cellulose from the biomass is important in the final properties of the resulting composites.[27]

The aim of the present article is to process and characterize the mechanical behavior and water uptake of PP/lignocellulosic residual softwood fiber composites. The influence of the steam-explosion pretreatment of the filler on the composite performance is described, as well as the effect of the treatment of the filler with a graft copolymer of PP, maleic anhydride PP (MAPP), used as coupling agent to promote adhesion between both components.

EXPERIMENTAL

Materials

Polymeric Matrix

Polypropylene (PP) was provided as pellets by APPRYL. Its melting temperature was experimentally determined by differencial scanning calorimetry (DSC) (10°C/min) and was T_m = 173°C. Its degree of isotacticity was between 93 and 98% and its density at room temperature was 0.905 g/cm^3.

Compatibilizing Agent

A commercially available maleic anhydride–polypropylene copolymer (MAPP) (ELF-ATOCHEM) was used as a coupling agent for fiber treatment. It contained 1 wt % of maleic anhydride and was expected to improve the compatibility and adhesion between the lignocellulosic fiber and the PP matrix.

Filler

The experiments were carried out using a mixture of softwood residues, spruce (*Abies alba*), and

Table I Average Chemical Composition and 95% Confidence Interval of the Raw Mixture of Softwood Residues

Constituent	Content (wt %)
Ash	0.4 ± 0.1
Hot water extractives	7.4 ± 1.4
Ethanol/toluene extractives	3.3 ± 1.4
Klason lignin	25.1 ± 0.8
Glucose	38.2 ± 0.7
Other sugars[a]	28.5 ± 1.6

Results are based on 100 g of dry solid basis (%DSB).
[a] Other sugars represent xylose, galactose, arabinose and mannose.

pine (*Pinus insignis*), harvested in Lleida, Catalonia, in the northeast of Spain. The ground material was sieved to 100 mesh (0.150 mm). Table I shows the average chemical composition of the raw material. The original and pretreated substrates were chemically analyzed using the following standard methods: ASTM E-871-82 for moisture content; ASTM D-3516-76 for ash content; ASTM D-1111-84 for hot-water extractives. Klason lignin was measured using the ASTM D-1106-84 method. Carbohydrates were analyzed by HPLC.[28] The measurement of the degree of polymerization (DP_v) of the cellulosic fibers was reported elsewhere.[29]

Pretreatment of the Lignocellulosic Filler

The hydrolytic pretreatment was carried out in a continuous tubular reactor described elsewhere.[30] It is capable of processing up to 100 kg · h^{-1} of aqueous suspension with a solid consistency of 7 wt %. The R_o severity factor, which groups the treatment temperature and time into a single variable, was used to characterize the severity of the steam explosion treatment.[31] Table II reports the pretreatment conditions, yield, as well as the chemical composition and codification of the different fibers.

Sieve Analysis

Particle size and particle-size distributions of lignocellulosic fibers were obtained from dynamic light scattering (quasielastic light scattering) with a MALVERN MasterSizer X instrument. It allows one to obtain the particle mean diameter of the fibers assimilated to spherical particles, and the apparent specific surface of the particles. The diluted fiber suspension was set in a cell and exposed to a monochromatic low power helium–neon laser beam (λ = 632.8 nm). The detector was a solid-state silicon photodiode array detector. Particles shift under the brownian motion and oscillate around an equilibrium position. Intensity fluctuations scattered at 90° are amplified and used to determine the diffusion coefficient. The particle mean diameter was calculated from the Stokes-Einstein equation.

Polypropylene/Lignocellulosic Composites

A Brabender FDO 234H model was used to mix and compound lignocellulosic fibers with the polymeric matrix. The fibers were previously dried at 105°C. The treatment of the different kinds of fibers was carried out by coating the surface of fibers with MAPP in a proportion of 0.3 wt % of maleic anhydride groups. Mixing was done at 190°C for 10 min using a rotor speed of 90 rpm. Raw and treated fibers were mixed with PP at 200°C for 10 min with a rotor speed of 90 rpm. Composite materials with fibers content ranging from 0 to 60 wt % were prepared. The evaluation of the steam explosion step effect was carried out with composite materials filled using 20 wt % of lignocellulosic fibers. The volume fraction, ϕ_f, of fiber was calculated from the weight fraction, w_f, using:

$$\phi_f = \frac{w_f/\rho_f}{w_f/\rho_f + (1 - w_f)/\rho_m} \quad (1)$$

Table II Pretreatment Conditions, Yield, and Chemical Composition of the Different Fibers

Fiber Codification	F1	F2	F3
Experimental conditions			
Temperature (°C)	176	215	220
Time (min)	2.5	3.0	2.1
Log R_o	2.6	3.9	3.9
Acid addition	—	—	0.4
log R_{OH}	1.1	1.5	1.8
Total solubilization	17.5	29.3	34.8
Fiber composition:			
Alfa-cellulose	39.4	33.4	22.4
DP_v	630	450	300
Anhydre glucose	35.6	36.6	34.9
Other sugars[a]	17.7	10.6	1.2
Klason lignin	24.0	21.4	20.2
Organic extractives	3.3	3.0	4.9

Results are based on 100 g of dry solid basis (%DSB).
[a] Other sugars represents xylose, galactose, arabinose and mannose.

where, ρ_f and ρ_m are the density of the filler ($\sim$ 1.5) and of the matrix ($\sim$ 0.905), respectively. After mixing, the mixture was then extruded in a Max Mixing Extruder CSI CS 194 model at 190°C, with a rotor speed of 270 rpm. This extrusion step was performed twice. Granulation was carried out to obtain pellets 3.2 mm in diameter and around 3–4 mm in length. Specimens for mechanical properties evaluation and water absorption experiments were made by compression molding the composites. The compounded and extruded pellets were hot pressed with a CARVER Laboratory Press at 14 MPa for 15 min at 190°C.

Methods

Inverse Gas Chromatography

Inverse gas chromatography (IGC) experiments were carried out to determine the surface energy and the acid-base specific interactions of the fiber surface. For the IGC probing, about 0.4 g of material (stationary phase) was packed into a glass tube 6 mm diameter and 250 mm long, and conditioned overnight at 105°C under a flow of dry nitrogen. A DELSI 121 DFL gas chromatograph equipped with a flame ionization detector was used to measure the retention times. The dispersive component of the surface energy of the samples was determined using a series of *n*-alkane probes from C_6 to C_9. The acid/base interactions were evaluated using tetrahydrofuran and chloroform as polar probes. The column was set at a temperature of 70°C and the injector and the detector at 170°C. Nitrogen was used as the carrier gas with a flow of 0.07 $mL \cdot s^{-1}$ and methane was used to determine the dead volume. The injections were done at infinite dilution. The IGC method for the calculation of the dispersive component of the surface energy of a solid, and of the acid/base properties of its surface were described in detail elsewhere.[32–37]

Scanning Electron Microscopy

Scanning electron microscopy (SEM) was performed to investigate the morphology of the different kinds of fibers, and the interface between the filler and the matrix with a JEOL JSM-6100 instrument. The specimens were frozen under liquid nitrogen, then fractured, mounted, coated with gold/palladium on a JEOL JFC-1100E ion sputter coater, and observed. SEM micrographs were obtained using 7 kV secondary electrons.

Dynamic Mechanical Analysis

Dynamic mechanical tests were carried out with a Rheometrics RSA2 spectrometer in the tensile mode. Test conditions were chosen in such a way that the measurements were in the linear viscoelasticity region (the maximum strain ε was around 10^{-4}). The specimen was a thin rectangular strip with dimensions of 30 $\times$ 5 $\times$ 1 mm. Measurements were performed in isochronal conditions at 1 Hz, and the temperature was varied between 200 and 500 K by steps of 3 K. The setup measures the complex tensile modulus E^*, i.e., the storage component E' and the loss component E'', as well as tan ϕ ($= E''/E'$).

Tensile Tests

The nonlinear mechanical behavior of lignocellulosic fibers/PP composites was analyzed using an Instron 4301 testing machine in tensile mode, with a load cell of 100 *N* capacity. The specimen was a thin rectangular strip ($\sim$ 30 $\times$ 5 $\times$ 1 mm). Tensile tests were performed at a strain rate $\dot{\varepsilon} = 1.7 \times 10^{-3}\ s^{-1}$ (crosshead speed = 1 mm/min) and at 25°C. The nominal strain ε can be determined by $\varepsilon = (\ell - \ell_o)/\ell_o$, where ℓ and ℓ_o are the length during the test, and the length at zero time, respectively. The nominal stress σ was calculated by $\sigma = F/S_o$, where F is the applied load and S_o is the initial cross-sectional area. Stress vs. strain curves were plotted and Young's modulus (E) was measured from the low strain region.

Ultimate mechanical properties were also characterized. The nominal ultimate stress, or nominal stress at break (tensile strength), $\sigma_b = F_b/S_o$, where F_b is the applied load at break, were reported for each tested sample. Ultimate elongation was characterized by the nominal ultimate strain, or nominal strain at break, $\varepsilon_b = \Delta\ell_b/\ell_o$, where $\Delta\ell_b$ is the elongation at break. The values reported in this study are the average of at least six measurements and its 95% confidence interval.

Water Absorption

Wood is an hygroscopic material, but it is known that the steam-explosion process results in a remarkable increase of the extractable lignin and the almost complete elimination of hemicelluloses. These chemical changes decrease the water affinity of the fiber, and should results in a decrease of the moisture absorbance of the lignocellulosic filled composite. The specimen dimensions

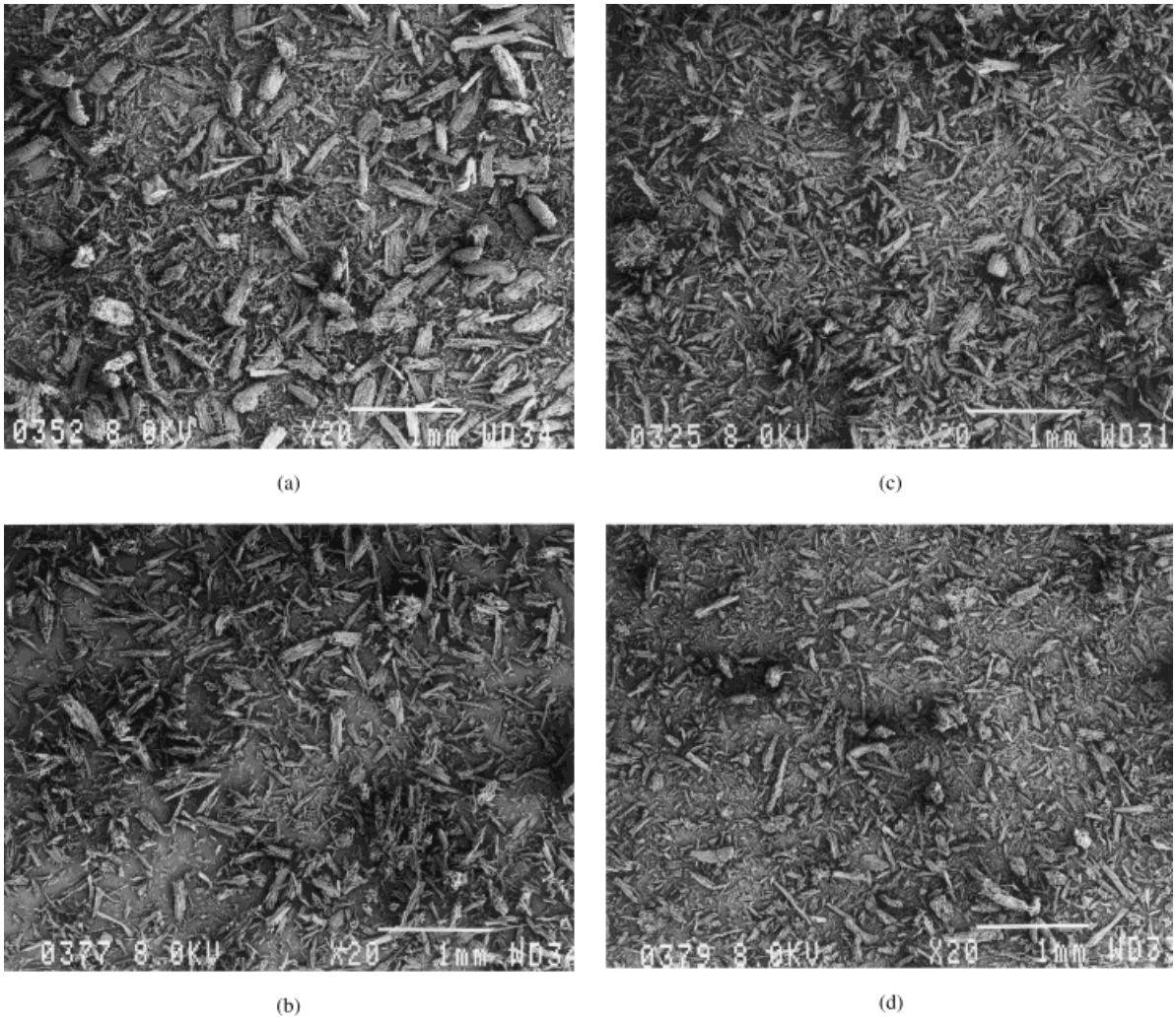

Figure 1 Scanning electron micrograph showing the different kinds of softwood fibers used in the present study: (a) raw fiber, (b) fiber F1, (c) fiber F2, (d) fiber F3.

for water uptake experiments were 10 × 10 × 1 mm. The composite films were supposed to be thin enough so that the molecular diffusion was considered to be one dimensional. A minimum of three samples were tested for each material.

Samples were first dried overnight at 70°C. They were subsequently cooled and weighted, and they were then immersed in distilled water, pH = 6 and 25°C. The samples were removed at specific intervals and blotted to remove the excess water on the surface. After weighting on a five-digit analytical balance, the weight percentage increase was calculated as follows:

$$\text{water uptake } (\%) = \frac{M_t - M_o}{M_o} \times 100 \qquad (2)$$

where M_t and M_o are the weights of the sample after t min exposure to water and before exposure to water, respectively.

RESULTS AND DISCUSSION

Morphological Characterization

Scanning electron microscopy (SEM) was used to characterize both the structure of lignocellulosic fillers and the morphology of PP-based filled composite materials.

Fiber Structure

The SEM micrographs in Figure 1 show the effect

of the pretreatment severity on the structure of the fibers. The pretreatment induces structural differences between the raw fiber [Fig. 1(a)] and the one pretreated at the lowest [fiber F1, Fig. 1(b)] or higher severity [fiber F2, Fig. 1(c)]. Raw filler presents unbroken and well-defined fibers. In the case of pretreated fibers, it can be noticed that the increase of pretreatment severity results in a loss of the fiber entirety and structure [Fig. 1(b) and (c)]. It also results in a shortening and in a thinning down of the fibers, which should have an influence on the mechanical behavior of resulting composites.[38] Both phenomena are due to the solubilization of the hemicellulosic fractions, cellulose and lignin.[39–41] Figure 1(c) and (d) displays the fiber surface of the fibers pretreated at log R_o = 3.9 uncatalyzed (fiber F2) and catalyzed with acid (fiber F3), respectively. The acidic treatments induces a decrease of the average fiber length. This shortening effect is better displayed at higher magnification. Figure 2 shows the raw filler and steam exploded and catalyzed with acid fibers (fiber F3). It is clear that the steam explosion process leads to a decrease of clustering of cellulose microfibrils. In addition, the surface of pretreated fibers is made of numerous shrinkage folds, and it becomes defibrillated as reported elsewhere by Kallavus and Gravitis.[42]

Composite Morphology

Figures 3 and 4 show SEMs of freshly fractured surface for a PP film filled with 20 wt % of softwood fibers using different kinds of fibers (raw fibers and fibers F3) and both untreated and MAPP-coated fibers. For each material, two different magnifications were used to display both the filler dispersion and interfacial adhesion.

Figures 3(a) and 4(a) correspond to untreated fibers in a PP matrix. They clearly indicate that the interfacial adhesion between the filler and matrix was poor, regardless of the steam-explosion pretreatment of the fiber. This can be readily seen from the absence of any physical contact between both components. The fibers are pulled out from the matrix and practically intact. Fracturing the sample did not lead to breaking the filler. In addition, holes and spacing occur in the matrix as well as along the fiber, resulting in poor contact and inferior stress transfer between the phases, as reported elsewhere for cellulose fiber-filled low-density polyethylene by Hedenberg and Gatenholm.[43]

Coating the fiber provided a good wetting, which can be observed from the near absence of

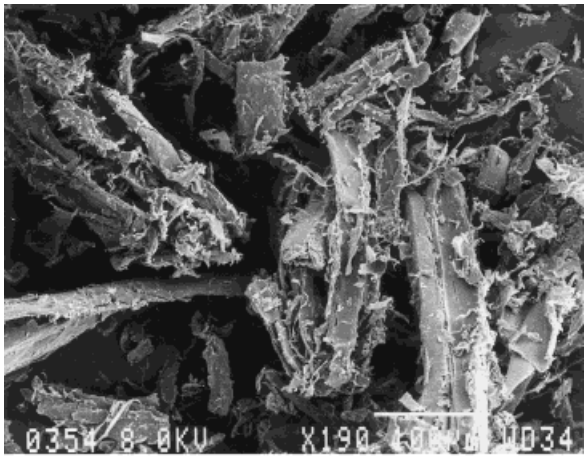

(a)

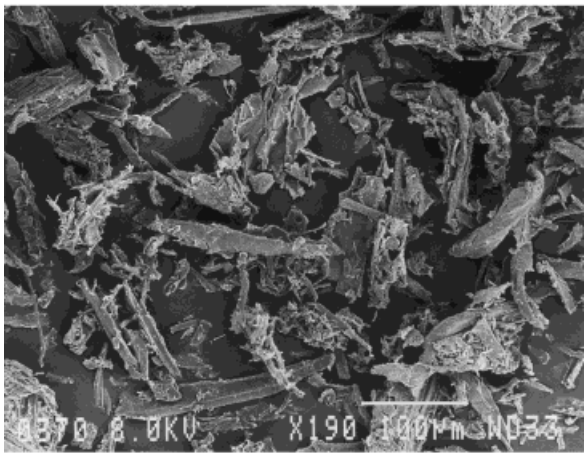

(b)

Figure 2 High magnification scanning electron micrograph of: (a) raw fiber, (b) fiber F3.

holes around the fillers and from the breaking of fillers during fracture [Figs. 3(b) and 4(b)]. In each case, the major component surrounding the modified fibers seems to be the continuous phase.

Another observation made by comparing high-magnification micrographs in Figures 3(a) and 4(a) is that the fiber surface is completely different. The raw fiber [Fig. 3(a)] is smooth, and the steam-explosion pretreated ones have a rough surface and a large reactive area due to the pretreatment, which is an important factor to enhance adhesion.[38]

Sieve Analysis

The mean diameter of softwood fibers assimilated to spherical particles was obtained from dynamic light-scattering measurements. Figure 5 shows

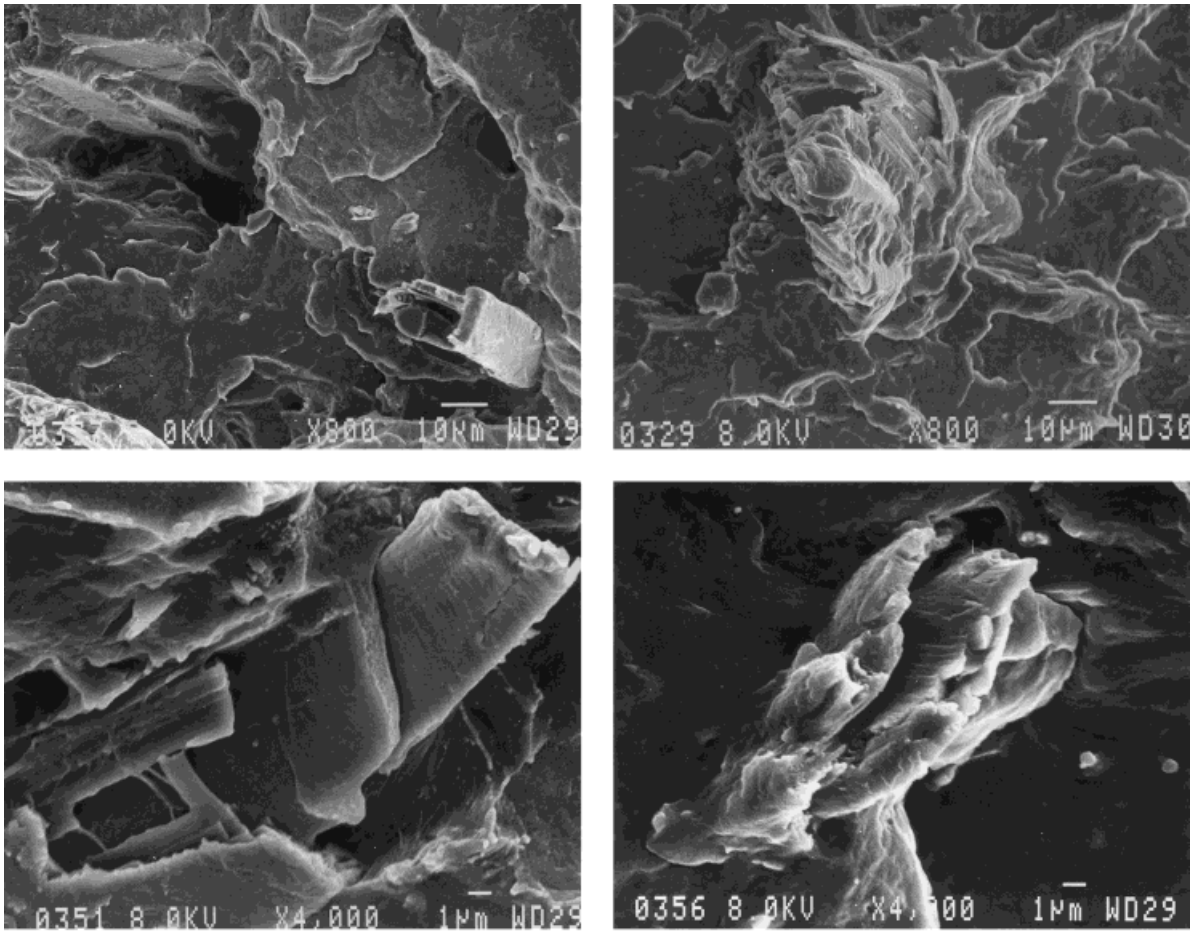

Figure 3 Scanning electron micrograph of freshly fractured surface for a PP film filled with 20 wt % of raw (a) untreated, and (b) MAPP-coated softwood fibers.

the evolution of the vol % of the particle vs. the particle diameter. Each filler displays a bimodal distribution. One peak is located around 50 μm, and the other one around 250 μm. They are assigned to more or less close packing of cellulose microfibrils. As the severity of the steam explosion pretreatment increases, the mean particle diameter decreases, and the magnitude of the peak associated to the higher diameter decreases, whereas the one related to the lower diameter increases. This result agrees with SEM observations. The apparent specific surfaces of the raw fiber and pretreated ones are reported in Table III. It increases as the severity of the steam-explosion pretreatment increases.

Surface Energy

Inverse gas chromatography (IGC) experiments were carried out to determine the surface energy and the acid-base specific interactions of each filler. The results of the surface energy and the polar interactions as well as some surface energy values found in the literature[32,35,44–48] are reported in Table III. It can be seen that the surface energy increases when steam-explosion pretreatment conditions increase, but it is worthy to notice that the fiber that had been catalyzed with acid presents an intermediate surface energy. Our results agree with those reported in the literature. The surface energy values of raw fibers of different lignocellulosic materials range between 24 and 31 mJ/m^2, which are similar to our result for softwood fiber (22 mJ/m^2). For the thermomechanical pulp (TMP), the surface energy ranges between 36 and 43 mJ/m^2, and for the chemithermomechanical pulp (CTMP), it is 36 mJ/m^2. So the pretreatment step modifies the surface of the fiber and one of the effects of this modification is

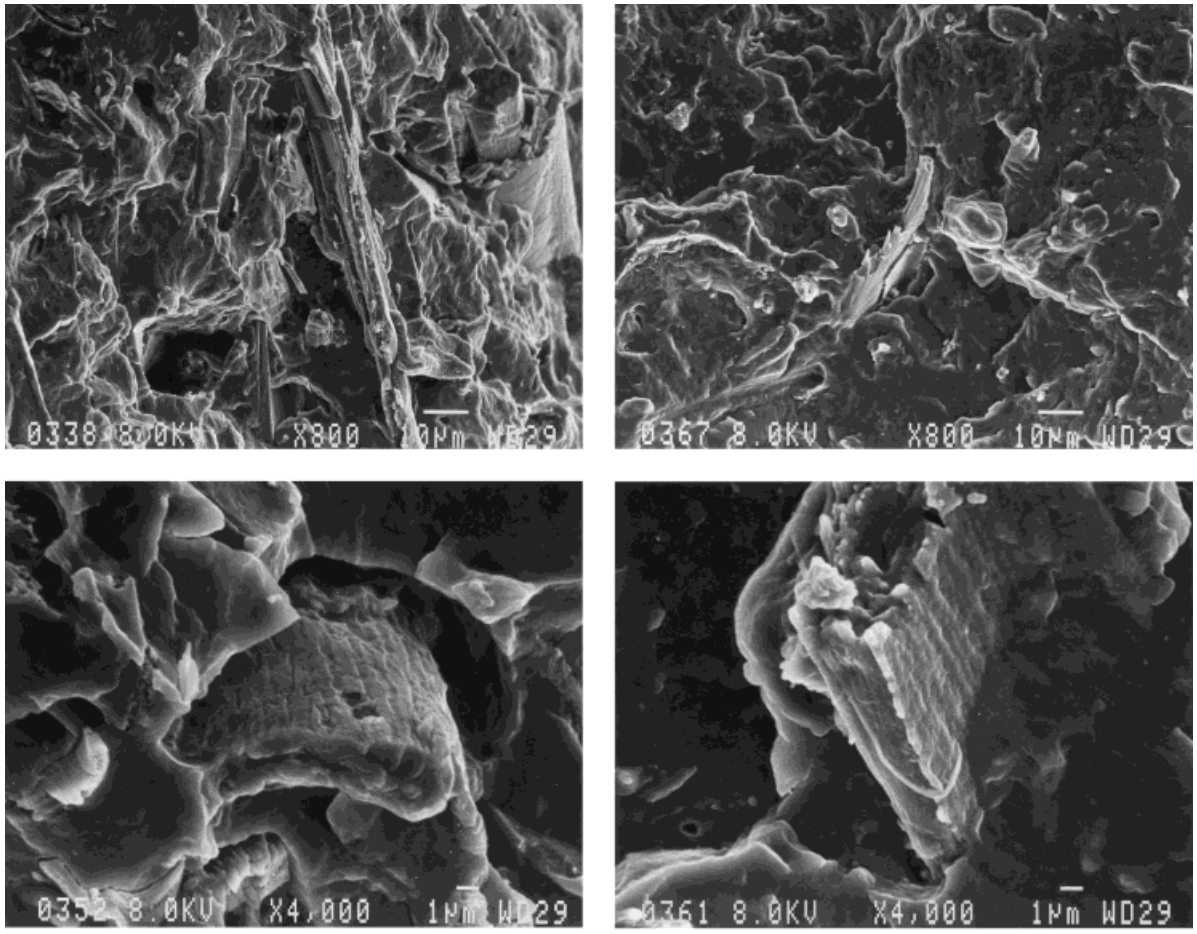

Figure 4 Scanning electron micrograph of freshly fractured surface for a PP film filled with 20 wt % of (a) untreated, and (b) MAPP-coated pretreated softwood fibers F3.

the increase of the surface energy. The PP matrix presents an intermediate surface energy, which is 33 mJ/m^2.[44]

The acidic character, displayed through the polar interactions, of the fiber increases with increasing pretreatment conditions. As expected, the fiber with the highest acidic character is the fiber pretreated and catalyzed with acid (approximately twice of the original fiber).

Mechanical Behavior

The mechanical behavior of both untreated and grafted with MAPP lignocellulosics based composite materials was investigated in both linear conditions (dynamic mechanical measurements, strain smaller than 10^{-3}) and nonlinear conditions (tensile tests up to the break).

Dynamic Mechanical Analysis

Dynamic mechanical measurements were performed on composite materials filled with 20 wt % of lignocellulosic fibers to display the effect of the steam-explosion step. The curves of $\log(E'/\text{Pa})$ (storage tensile modulus) vs. temperature at 1 Hz are displayed in Figure 6(a) and 6(b), for untreated and MAPP-coated based composites, respectively. For low temperatures, it was difficult to observe any change in the modulus with variation in the fiber loading and pretreatment conditions. As it is well known, the exact determination of the glassy modulus depends on the precise knowledge of the sample dimensions. To minimize this effect, the elastic tensile modulus, E' at 200 K was normalized at 1 GPa for all the samples. This can be justified by the fact that the difference between the elastic modulus of the

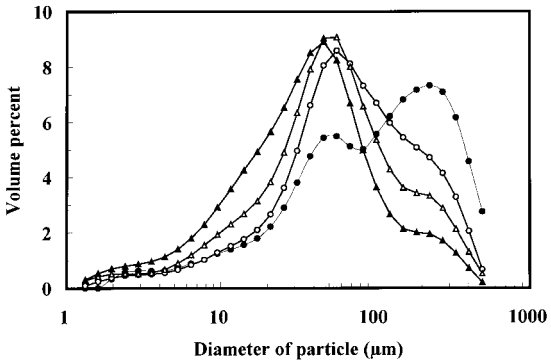

Figure 5 Volume percent of softwood fibers assimilated to spherical particles vs. particle diameter: raw fiber (●), fiber F1 (○), fiber F2 (△), fiber F3 (▲) (the solid lines serve to guide the eye).

glassy polymer and lignocellulosic filler was not high enough to easily appreciate any change.

The curves corresponding to the nonreinforced PP and PP/MAPP matrices are typical of semicrystalline thermoplastic behavior. The storage modulus remains practically constant up to the glass–rubber transition temperature (~ 270 K). At higher temperatures, a slight decrease in the elastic tensile modulus was observed, corresponding to the glass–rubber transition. This slight modulus drop corresponds to an energy dissipation displayed in a relaxation process where tan ϕ passes through a ill-defined maximum (not shown). This relaxation process, labeled α, involves cooperative motions of long amorphous chain sequences. The rubbery modulus is known to depend on the degree of crystallinity of the material. The crystalline regions act as physical crosslinks for the elastomer. In this physically crosslinked system, the crystalline regions would also act as filler particles due to their finite size, which would increase the modulus substantially. In the terminal zone, corresponding to the melting of crystalline domains (~ 450 K), the elastic tensile modulus becomes lower and lower with temperature, and the experimental setup fails to measure it.

The addition of 20 wt % of untreated or grafted with MAPP lignocellulosic fibers in the host PP polymer is displayed in Figures 6(a) and 6(b), respectively. Four kinds of filler were used, namely raw, F1, F2, and F3 fibers. It does not change significantly the modulus drop at the glass–rubber transition and the rubbery modulus, except when raw fibers and fibers F1 coated with MAPP were used. The expected reinforcing effect depends on two main factors: (1) the intimate adhesion between both components, which induces the efficiency of the stress transfer from

Table III Apparent Specific Surface, Surface Energy, and Polar Interactions of the Different Fibers and Values Found Reported from the Literature for Different Materials

	Apparent Specific Surface (m^2/g)	Surface Energy[a] (mJ/m^2)	Polar Interactions[b]
Material			
Raw fiber	0.1598	22 ± 2	1.27
Fiber F1	0.1800	37 ± 5	1.28
Fiber F2	0.2405	44 ± 9	1.72
Fiber F3	0.3152	34 ± 2	2.16
Literature values:			
Polypropylene[c] [44]	—	33	—
Oakwood[32]	—	27	—
Aspen[32]	—	24	—
Fir[32]	—	31	—
TMP[45]	—	36/43	—
CTMP[35]	—	36	—
Cellulose[46]	—	27	—
Cellulose[47,48]	—	43	—
Microcrystalline cellulose[47,48]	—	41	—

TMP: thermomechanical pulp; CTMP: chemithermomechanical pulp.
[a] Absolute value.
[b] Relative value.
[c] Measured at 60°C.

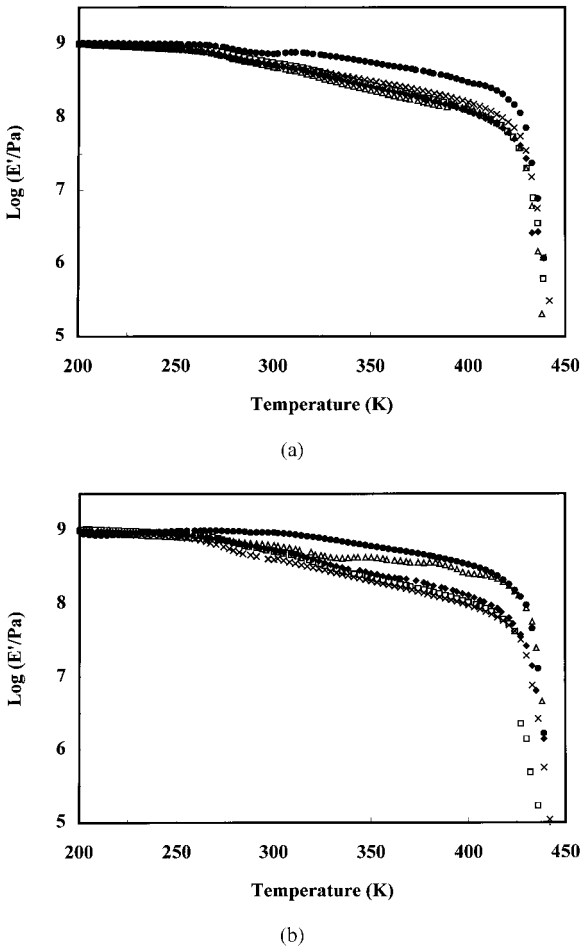

Figure 6 Storage tensile modulus E' vs. temperature at 1 Hz for softwood fiber-filled PP: pure matrix (□), 20 wt % of raw fiber (●), 20 wt % of fiber F1 (△), 20 wt % of fiber F2 (×), and 20 wt % of fiber F3 (◆). (a) Corresponds to untreated fibers, and (b) to MAPP-coated fibers.

the matrix to the fibers, and (2) the aspect ratio (L/d, L being the length and d the diameter) of the fiber. These two factors evolve in opposite way with the severity of the steam-explosion process. Harder pretreatment conditions induce higher surface energy, but decrease at the same time the aspect ratio. It seems from our experimental results that the influence of the aspect ratio play the major role on the mechanical behavior of PP-based composites.

In addition, it is worth noting that the temperature of the modulus drop associated with the melting of the PP matrix is unaffected by the addition of untreated softwood fibers, regardless of the steam-explosion pretreatment. Using fibers coated with MAPP, it appears at a higher temperature for composites than for pure matrix. The storage modulus is 1 MPa at ~ 430 K for the PP/MAPP matrix, and ~ 440 K for MAPP-coated softwood fiber-based composites. It is (~ 440 K) for the PP matrix, regardless of the untreated fiber loading and the pretreatment. This phenomenon can be ascribed to an interfacial effect, and to the anchoring of the polymeric chain on the lignocellulosic fiber surface during melting.

High Strain Behavior (Nonlinear Conditions)

The effect of fiber loading was first investigated using both untreated and MAPP-coated fibers F2. A typical stress vs. strain curve of a 20 wt % MAPP-coated fiber F2-reinforced PP composite is reported in Figure 7. The tensile or Young's modulus was determined from the slope of the stress vs. strain curves in the vicinity of $\sigma = \varepsilon = 0$, i.e., for $\varepsilon < 1\%$. Results are reported in Figure 8, which shows the evolution of the tensile modulus vs. the lignocellulosic fiber content. Open and full circles refer to the experimental data obtained with untreated and MAPP-coated fibers, respectively. MAPP modified matrix has a lower modulus than pure PP. The introduction of grafted MA monomer units within the PP main chain decreases the regularity of the macromolecular structure, which leads, in turn, to a lower degree of crystallinity.

For untreated fiber-filled systems (Fig. 8, open circles), the Young's modulus is almost independent of the lignocellulosic filler content and remains roughly constant, at least up to 60 wt %. No reinforcing effect is displayed for these composites. On the contrary, the tensile modulus in-

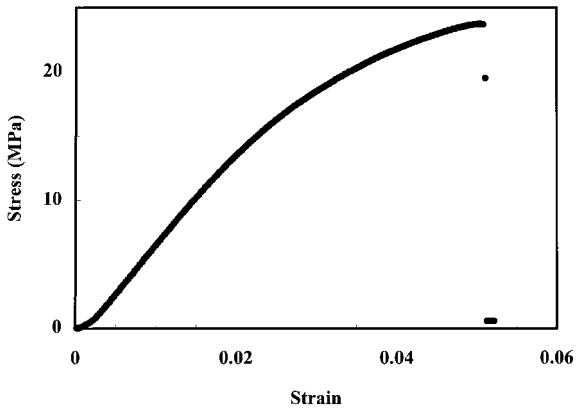

Figure 7 Typical stress vs. strain curve for a 20 wt % MAPP-coated fibers F2-reinforced polypropylene composite at 25°C, $\dot{\varepsilon} = 1.7 \times 10^{-3}\ s^{-1}$.

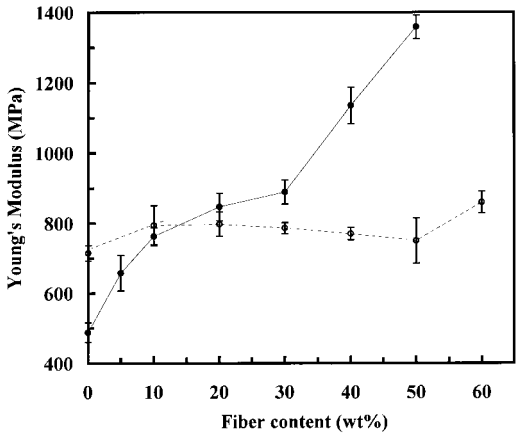

Figure 8 Young's Modulus of pretreated softwood fiber (fiber F2)-filled PP composites vs. fiber loading: untreated fibers (○), and MAPP-coated fibers (●) (the solid and dashed lines serve to guide the eye). Average values and 95% confidence interval of at least six tests are reported.

creases with filler content when MAPP is used to coat the fibers (Fig. 8, full circles). This result is ascribed to the beneficial effect of MA grafting to the PP backbone, which leads to an increase of the interfacial modulus. The interfacial modulus corresponds to the polymer modulus in the filler–matrix interphase. By definition, the interphase exists from some point in the filler where the local properties begin to change from the filler bulk properties, through the actual interface into the matrix where the local properties again equal the bulk properties. Three regions of modulus evolution are displayed in Figure 8, depending on the coated filler volume fraction range. For low loading (up to ~ 10 wt %) the modulus increases regularly from 488 to 762 MPa. At a higher filler content (up to ~ 30 wt %) it tends to stabilize or at least to show a lower increase rate. For a higher volume fraction (>30 wt %) the reinforcing effect increases again, and the modulus is 1.36 GPa for 50 wt % fiber loading.

In the literature, a number of theories and equations have been developed to predict the mechanical behavior of composite materials in terms of microstructure and fiber and matrix properties (see, e.g., ref. 50). Although these methods give satisfactory predictions of the mechanical properties for fiber-reinforced polymers, particularly moduli, they are usually only applicable to unidirectional fiber reinforcement. More rigorous calculations are also difficult to perform, and often require adjustable coefficients to be achieved.

The theoretical model of Halpin-Kardos[51] gives, in a relatively easy way, the elastic tensile modulus E_c of composites reinforced by randomly dispersed short fibers. In this approach, fibers are supposed to be dispersed in a continuous matrix, and no interaction between fillers is taken into account. The properties of the composite depend on the size, shape, and volume fraction of the filler and on the mechanical properties of both the matrix and the fibers. The composite is assimilated to a "quasi-isotropic" material framed by four layers of oriented plies (at 0°, 45°, 90°, and −45°).

The mechanical properties of a single ply (unidirectional short fibers) are given by the Halpin-Tsaï micromechanics equations ("self consistent" approach).[52] Details of the calculations can be found elsewhere.[15]

The Halpin-Kardos model has been used to predict the mechanical behavior of MAPP-coated fiber F2/PP composites. At room temperature, the different parameters used in this approach have the following values: $(L/d) \sim 10$ [order of magnitude estimated from SEM, Fig. 1(c)], $\nu_m = 0.4$ (the matrix being semicrystalline and amorphous domains being in the rubbery state), $E_m = 0.488$ GPa (experimental data observed for the pure MAPP matrix), $\nu_f = 0.3$ (cellulose being in the glassy state), $E_{11f} = 10$ GPa (experimental value obtained for steam-exploded poplar wood[53] and cotton[54]), $E_{22f} = 10$ GPa and $G_f = 5$ GPa.

Figure 9 displays the evolution of the lignocellulosics/MAPP composites modulus vs. fiber content. Full circles refer to the experimental data,

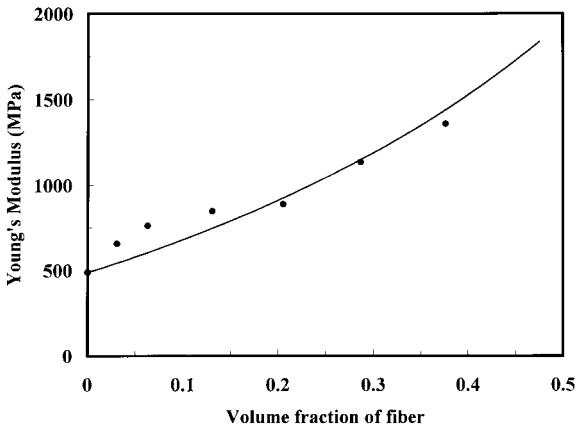

Figure 9 Young's Modulus of pretreated MAPP-coated softwood fiber (fiber F2)-filled PP composites vs. fiber loading: comparison between the experimental data (●) and predicted data from the Halpin-Kardos model (—).

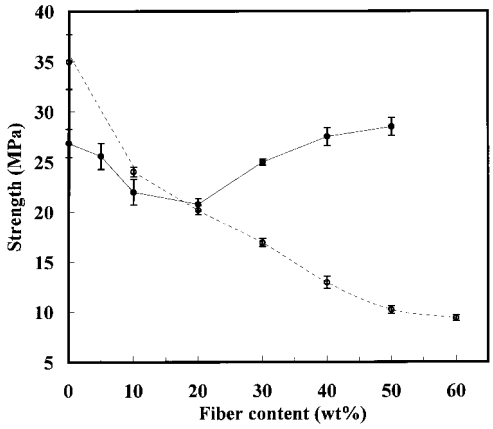

Figure 10 Tensile strength of pretreated softwood fiber (fiber F2)-filled PP composites vs. fiber loading: untreated fibers (○), and MAPP-coated fibers (●) (the solid and dashed lines serve to guide the eye). Average values and 95% confidence interval of at least six tests are reported.

whereas the solid line corresponds to the Halpin-Kardos prediction assuming the previous parameters. We ascertain that the estimated E_c values are in good agreement with the experimental data. A mean field approach allows one to predict the mechanical behavior of PP-filled treated fiber and to account for mechanical interactions within the composite.

Figure 10 shows the evolution of the tensile strength as a function of lignocellulosic filler content. It is higher for the unfilled PP matrix than for the MAPP matrix as a result of differences in the degree of crystallinity. The addition of untreated softwood fibers in the PP matrix affects the tensile strength of the composite. It decreases regularly from 35 MPa for the unfilled system down to 10 MPa for the 60 wt %-filled system. This phenomenon is due to a crazing effect or to a dewetting effect in which the adhesion between the filler and the matrix is destroyed, leading to a weakening of the interface strength. It agrees with morphological observations by SEM. The poor dispersion of the fibers and reduced interfacial adhesion to the polymer matrix may explain this reduction, because the effective transfer of stress between matrix and filler requires an adequate interfacial bonding.[55,56] The stress is transferred from the matrix to the fibers through the interfacial shear stress. This stress is concentrated at the fiber ends. With the increase in strain, these are the sites where the interface first fails and debonding of fibers and matrix (shear failure of the matrix) begins. The magnitude of this interfacial shear strength is determined by three factors: (1) the strength of the chemical bond between the fibers and the matrix; (2) the friction between the fibers and the matrix, resulting from pressure exerted on the fibers by the matrix; and (3) the shear strength of the matrix.[56] The lack of intimate adhesion between both components leads to numerous irregularly shaped microvoids or microflaws in the composite structure. Because of these microflaws the transfer of stress from the matrix to the fibers is poor, and the mechanical properties of the fibers are not fully utilized.

This trend is changed using an adhesion promoter such as MA, which change the adhesion and the nature of the filler–polymer interface (Fig. 10). For MAPP-coated fiber-filled systems, the tensile strength first decreases with fiber loading from 27 to 21 MPa for the unfilled and 20 wt %-filled material, respectively. For higher fiber content, the tensile strength increases up to 29 MPa. In the case of fiber-reinforced composites, it is well known that there exists a critical aspect ratio at which the mechanical properties of the composites are maximized. This critical aspect ratio depends on the volume fraction of the fiber and also on the ratio of the modulus of fiber to the matrix modulus.[57] At low fiber loading the fibers play no major role, and the strength of the composite is matrix dominated. The strength of the composite was found to increase above a critical volume fraction of filler, which in fact, depends on the aspect ratio. The critical volume fraction was found to decrease with increase in aspect ratio.

Figure 11 shows the evolution of the elongation at break vs. filler content. PP- and MAPP-modified PP display a ductile behavior at room temperature, with elongation at break of 47 and 40%, respectively. Fillers cause a dramatic decrease in elongation at break, and PP-based composites display a brittle behavior with only a few percent of filler. It breaks for ε lower than 10% when only 5 wt % of fillers were included in PP. This well-known decrease in elongation at break with rigid fillers arises from the fact that the actual elongation experienced by the polymer matrix is much higher than the measured elongation of the specimen. No distinct difference is observed when functionalized compatibilizer, MAPP, is added.

The evaluation of the steam explosion step effect was carried out using composite materials containing 20 wt % of lignocellulosic fibers. Figure 12(a) displays the evolution of the relative tensile

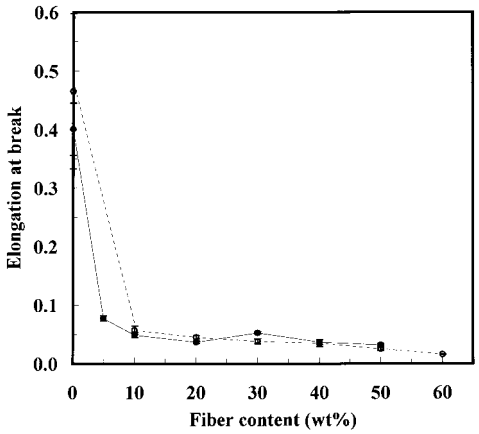

Figure 11 Elongation at break of pretreated softwood fiber (fiber F2)-filled PP composites vs. fiber loading: untreated fibers (○), and MAPP-coated fibers (●) (the solid and dashed lines serve to guide the eye). Average values and 95% confidence interval of at least six tests are reported.

modulus, i.e., the modulus of the composite divided by the one of the pure matrix, as a function of the steam-explosion severity for both untreated and MAPP-coated fiber-filled composites. By comparing the different untreated fiber-filled composites (white bars), it is observed that the lowest steam-explosion pretreatment severity (fiber F1) leads to a decrease of Young's modulus. This result agrees with dynamic mechanical analysis measurements at room temperature [Fig. 6(a)], and can be ascribed to the shortening of the fiber with pretreatment. As the steam explosion pretreatment severity increases (fibers F2 and F3) the relative Young's modulus is enhanced compared to the one of fiber F1-based composite. It seems that the shortening effect of the fiber becomes negligible with respect to the increase in polar interaction component of the surface energy.

When fibers are coated with MAPP (stripped bars), the relative Young's modulus of the composite increases, regardless of the steam-explosion pretreatment severity. This is ascribed, as previously shown, to the effectiveness of the bonding of the functionalized compabilizer, MAPP, to cellulose, and to the increase of the interfacial modulus. In addition, it is worth noting that the same trend as for the untreated fiber-based composites is observed, i.e., a decrease for lower pretreatment severity followed by an increase when the severity augments.

Figure 12(b) shows the relative strength vs. steam-explosion severity. No distinct difference is observed for untreated fiber-based composites. The relative tensile strength is around 0.6, whatever the steam explosion severity was. However, when MAPP is added, each material displays a higher relative tensile strength. This again confirms that the grafting really occurs, and that this treatment improves wetting of the wood fiber by polypropylene.[32]

Water Absorption

The water uptake during exposure to water of steam-exploded softwood fiber F2-filled PP is plotted against time in Figure 13. Figure 13(a) corresponds to untreated fiber-based materials, and

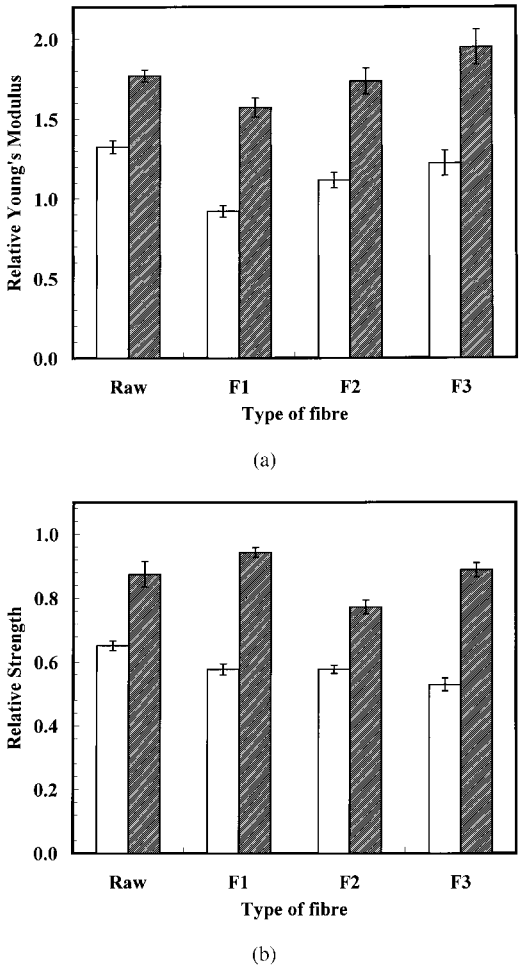

Figure 12 (a) Relative Young's Modulus, and (b) relative strength of the 20 wt % filled composites with different kinds of fiber. Untreated fiber-filled PP composites are in white bars and MAPP-coated fibers filled PP composites are in stripped bars. Average values and 95% confidence interval of at least six tests are reported.

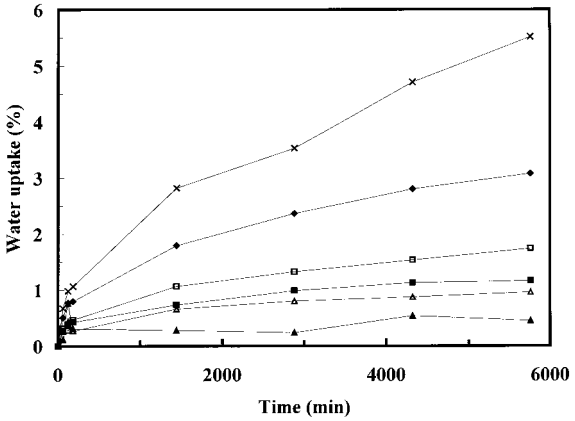

(a)

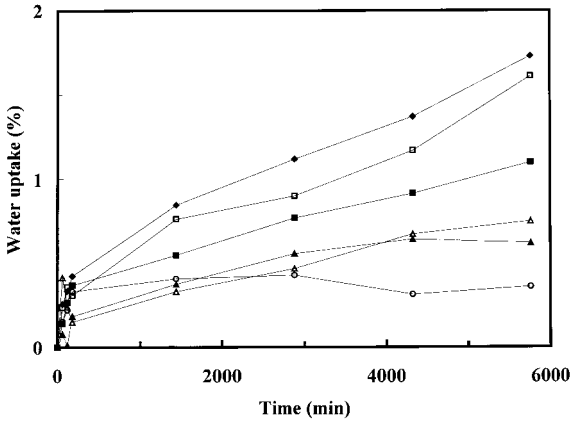

(b)

Figure 13 Percent water uptake during exposure to water vs. time for composites filled with 5 (○), 10 (▲), 20 (△), 30 (■), 40 (□), 50 (◆), and 60 wt % (×) of (a) untreated, and (b) MAPP-coated softwood fibers (the solid lines serve to guide the eye).

Figure 13(b) corresponds to MAPP-coated fiber composites. These swelling data are means of three trials, and the reliability of measurements was very good. We ascertain that each composition absorbs water during the experiment, but following different behaviors. Two sorption rates are displayed in both Figure 13(a) and 13(b). At lower times, the kinetic of absorption is fast, whereas long-time kinetic of absorption is slow and leads to a plateau, at least for low fiber loading compositions. The maximum relative water uptake, ascribed to the longer time experimental data in Figure 13, increases with the hygroscopic filler content, as reported elsewhere for microcrystalline starch-reinforced thermoplastic.[18] However, the water uptake remains relatively low, regardless of the sample composition.

This maximum relative water uptake is strongly affected by the MAPP coating treatment of the fiber. For instance, it is around 3.1 wt % for untreated fiber-based system and 1.7 wt % for the treated fiber composite, when the fiber loading is 50 wt %. This result can be analyzed in relation with SEM observations and mechanical properties, and can be ascribed to an interfacial effect. It is likely that the excess of absorbed water in the untreated fiber-filled composite with respect to the MAPP-treated one displays clusters of water molecules at the interface due to the presence of microcavities. Indeed, it is well known that the interface between the matrix and filler in composites is an ill-defined but extremely important part of the material, which can easily allow the absorption of water. The encapsulation of the fiber with MAPP decreases the water sensitivity of the composite. During the coating, MAPP reacts with the hydroxyl groups of the lignocellulosic fibers to form covalent bonds that are more resistant to water penetration.[32,58] Similar results were obtained for epoxy resin–glass beads systems using both raw and silane treated beads.[59]

The water uptake of soaked samples was also measured as a function of steam-explosion pretreatment for 20 wt %-filled systems. Results are reported in Table IV. It can be observed that the highest absorption values correspond to the composites filled with the fiber pretreated with the lowest severity (Fiber F1, Log R_o = 2.6), regardless of the surface treatment of the fiber. Higher pretreatment severity induces a lower absorption level, probably due to chemical changes caused by the pretreatment and removal of part of the hemicelluloses.

Table IV Water Uptake of 20 wt % Softwood Fiber-Filled PP after 72 h Exposure to Distilled Water at Room Temperature

Fiber	F1	F2	F3	F1	F2	F3
Treatment		untreated			MAPP coated	
Water uptake (wt %)	1.05	0.68	0.33	0.87	0.48	0.46

CONCLUSIONS

Composite materials were obtained by compounding and molding steam-exploded residual softwood and polypropylene. The steam-explosion pretreatment severity increased the surface energy and the apparent specific surface, but at the same time decreased the aspect ratio of the fiber. Steam-exploded softwood was found to be ineffective, giving similar Young's modulus and lower strengths compared to the unfilled PP matrix and to the composites with raw softwood fibers. Both the tensile strength and the Young's modulus of the composites increased when a functionalized compatibilizer, MAPP, was used to coat the fibers. The elongation at break value, however, remained almost same for both untreated and MAPP-treated fiber composites. The improvement in tensile strength and modulus was attributed to the better adhesion between the treated fiber and PP. This was supported by SEM observation of the fractured surface of untreated softwood fiber composites and MAPP-coated fiber composites. The reinforcing effect of MAPP-treated filled PP was well predicted from a model based on a mean field approach (Halpin-Kardos model). Lignocellulosics being highly hygroscopic materials, the water uptake was characterized as a function of the composite composition for both untreated and MAPP-coated fibers. It was found that the composite absorbs more water as the fiber loading is higher. Moisture absorbance can be prevented if the softwood fiber is thoroughly encapsulated in a MAPP coating as a result of the better adhesion between matrix and filler. Optimum bonding is, therefore, responsible for maximum static and dynamic mechanical properties and environmental resistance.

The authors gratefully acknowledge Mrs C. Bonini and Mr M. Paillet for their help in film processing, Prof. A. Gandini and Dr. G. Depres for valuable assistance in IGC experiments, and Mrs D. Dupeyre for her help in SEM. The authors are indebted to the Spanish Government and the Generalitat de Catalunya (Catalan Local Government) for financial support, project number GSR96 for quality groups and project number QFN95-4720, and a Grant of the Universitat Rovira i Virgili (Catalunya).

REFERENCES

1. Klason, C.; Kubat, J.; Strömvall, H. E. Int J Polym Mater 1984, 10, 159.
2. Zadorecki, P.; Michell, A. J. Polym Compos 1989, 10, 69.
3. Maldas, D.; Kokta, B. V.; Daneault, C. Int J Polym Mater 1989, 12, 297.
4. Maldas, D.; Kokta, B. V.; Daneault, C. J Appl Polym Sci 1989, 38, 413.
5. Raj, R. G.; Kokta, B. V.; Groleau, G.; Daneault, C. Plast Rubber Process Appl 1989, 11, 215.
6. Raj, R. G.; Kokta, B. V.; Maldas, D.; Daneault, C. J Appl Polym Sci 1989, 37, 1089.
7. Chtourou, H.; Riedl, B.; Ait-Kadi, A. J Reinf Plast Compos 1992, 11, 372.
8. Raj, R. G.; Kokta, B. V.; Nizio, J. D. J Appl Polym Sci 1992, 45, 91.
9. Sanadi, A. R.; Caufield, D. F.; Jacobson, R. E.; Rowell, R. M. Ind Eng Chem Res 1995, 34, 1889.
10. Sanadi, A. R.; Prasad, S. V.; Rohatgi, P. K. J Sci Ind Res 1985, 44, 437.
11. Sanadi, A. R.; Rowell, R. M.; Caulfield, D. F. Polym News 1996, 20, 7.
12. Boldizar, A.; Klason, C.; Kubat, J.; Näslund, P.; Saha, P. Int J Polym Mater 1987, 11, 229.
13. Dufresne, A.; Vignon, M. R. Macromolecules 1998, 31, 2693.
14. Favier, V.; Canova, G. R.; Cavaillé, J. Y.; Chanzy, H.; Dufresne, A.; Gauthier, C. Polym Adv Technol 1995, 6, 351.
15. Helbert, W.; Cavaillé, J. Y.; Dufresne, A. Polym Compos 1996, 17, 604.
16. Dufresne, A.; Cavaillé, J. Y.; Helbert, W. Polym Compos 1997, 18, 198.
17. Dufresne, A.; Cavaillé, J. Y.; Helbert, W. Macromolecules 1996, 29, 7624.
18. Dufresne, A.; Cavaillé, J. Y. J Polym Sci Polym Phys 1998, 36, 2211.
19. Mason, W. H. Paper Trade J 1927, 55, 131.
20. Asplund, A. Svensk Paperstiding 1953, 56, 550.
21. Delong, E. A. Can. Pat. 1096374 (1978).
22. Koran, Z.; Kokta, B. V.; Valade, J.-L.; Law, K. N. Pulp Paper Can 1979, 3, T107.
23. Asplund, A. U.S. Pat. 4136207 (1979).
24. Marchessault, R. H.; Coulombe, S.; Morikawe, H.; Robert, D. Can J Chem 1981, 60, 237.
25. Excoffier, G.; Toussaint, B.; Vignon, M. R. Biotechnol Bioeng 1991, 38, 1308.
26. Beltrame, P. L.; Carniti, P.; Visciglio, A.; Focher, B.; Marzetti, A. Bioresources Technol 1992, 39, 165.
27. Dufresne, A.; Cavaillé, J. Y.; Vignon, M. R. J Appl Polym Sci 1997, 6, 1185.
28. Saeman, J. F.; Bubl, J. L.; Harris, E. E. Ind Eng Chem 1945, 17, 35.
29. Martinez, J. M.; Reguant, J.; Montero, M. A.; Montané, D.; Salvado, J.; Farriol, X. Ind Eng Chem Res 1997, 36, 688.
30. Montané, D.; Salvado, J.; Farriol, X.; Chornet, E. Biomass Bioenergy 1993, 4, 427.

31. Overend, R. P.; Chornet, E. Philos Trans R Soc Lond 1987, A321, 523.
32. Coupas, A. C.; Gauthier, H.; Gauthier, R. Polym Compos 1998, 19, 280.
33. Simonsen, J.; Hong, Z.; Rials, T. G. Wood Fiber Sci 1997, 29, 75.
34. Chtourou, H.; Riedl, B.; Kokta, B. V. J Adhesion Sci Technol 1995, 9, 551.
35. Kandem, D. P.; Riedl, B. J Colloid Interface Sci 1992, 150, 507.
36. Riedl, B.; Kandem, P. D. J Adhesion Sci Technol 1992, 6, 1053.
37. Lavielle, L. Ann Phys Fr 1989, 14, 1.
38. River, B. H.; Vick, C. B.; Gillespie, R. H. In Wood as an Adherent. Treatise on Adhesion and Adhesives; Minford, J. D., Ed.; Marcel Dekker: New York, 1991, vol. 7.
39. Anglès, M. N.; Reguant, J.; Martinez, J. M.; Farriol, X.; Montané, D.; Salvadó, J. Biotechnology 1997, 59, 185.
40. Reguant, J.; Martinez, J. M.; Montané, D.; Salvadó, J.; Farriol, X. J Wood Chem Technol 1997, 17, 91.
41. Vignon, M. R.; Dupeyre, D.; Garcia-Jaldon, C. Biotechnology 1996, 58, 203.
42. Kallavus, U.; Gravitis, J. Holzforschung 1995, 49, 182.
43. Hedenberg, P.; Gatenholm, P. J Appl Polym Sci 1995, 56, 641.
44. Felix, J. M.; Gatenholm, P. J Appl Polym Sci 1991, 42, 609.
45. Doris, G. M. Ph.D. Thesis, McGill University, Montreal, Canada (1979).
46. Westerlind, B. S.; Berg, J. C. J Appl Polym Sci 1988, 36, 523.
47. Lee, H. L.; Luner, P. J Colloid Interface Sci 1991, 146, 195.
48. Lee, H. L.; Luner, P. Tappi 1972, 55, 116.
49. Drzal, L. T. Adv Polym Sci 1985, 75, 1.
50. Hull, D. In An Introduction to Composite Materials; Cambridge University Press: Cambridge, 1981.
51. Halpin, J. C.; Kardos, J. L. J Appl Phys 1972, 43, 2235.
52. Tsaï, S. W.; Halpin, J. C.; Pagano, N. J. Composite Materials Workshop; Technomic: Stamford, CN, 1968.
53. Focher, B.; Marzetti, A.; Conio, G.; Marsano, E.; Cosani, A.; Terbojevich, M. J Appl Polym Sci 1994, 51, 583.
54. Brandrup, J.; Immergut, E. H. In Polymer Handbook; John Wiley & Sons: New York, 1989, 3rd ed.
55. Maiti, S. N.; Singh, K. J Appl Polym Sci 1986, 32, 4285.
56. McCrum, N. G.; Buckley, C. P.; Bucknall, B. In Principles of Polymer Engineering; Oxford University Press: New York, 1988.
57. Termonia, Y. J Mater Sci 1987, 22, 504.
58. Sean, T.; Sanschagrin, B.; Kokta, B. V.; Maldas, D. Makuzai Gakkaishi 1990, 36, 637.
59. Dufresne, A.; Lacabanne, C. Polymer 1995, 36, 4417.